Plastic Deformation of Vanadium Single Crystals during High-Dose Arsenic-Ion Implantation

O. Meyer and A. Azzam[(a)]

Kernforschungszentrum Karlsruhe, Institut für Nukleare Festkörperphysik, D-7500 Karlsruhe, Federal Republic of Germany

(Received 7 February 1984)

Implantation of As ions into (111) surfaces of V single crystals at room temperature results in the formation of supersaturated solid solution. Channeling studies revealed that at 14 at.% As the implanted region starts to rotate with respect to the bulk. The angle of rotation is perpendicular to a (110) plane, the slip plane, and increases with increasing As concentration. At 20 at.% As polygonization of the implanted region occurs. Results from (110) surfaces support the assumption that the implantation process causes a slip mechanism which gives rise to the rotation and the polygonization of the implanted layer.

PACS numbers: 61.70.Tm

High-dose ion implantation is a well-known technique to produce supersaturated interstitial and substitutional alloys in near-surface regions of materials.[1] The formation of crystalline intermetallic compounds of high lattice symmetry as well as amorphization has also been observed by implantation and irradiation.[2,3] Thermal activation of implanted mixtures may lead to intermediate metastable phases.[4]

In this work we report on the effect of plastic deformation and polygonization which may occur during high-dose ion implantation. The effect of polygonization during thermal activation of a high-dose implanted layer has been recognized in an earlier study[5]; however, it was treated in more detail in a recent work on high-dose Ga ion implantation (up to 35 at.%) in V single crystals.[4]

In the following work we will present results which show that plastic deformation and polygonization can occur already during the process of ion implantation at room temperature.

Vanadium single crystals were cut perpendicular to the $\langle 111\rangle$ and $\langle 110\rangle$ direction, lapped and etched as described elsewhere,[5] and homogeneously implanted with arsenic ions over a depth of 120 nm using four different energies (60, 120, 200, 300 keV) and fluences (7.9×10^{14}, 1.3×10^{15}, 1.3×10^{15}, 3.6×10^{15} $\mathrm{As}^+/\mathrm{cm}^2$ for 1 at.% As). X-ray diffraction spectra of the implanted surfaces were taken after polygonization using the Cu $K\alpha_1$ radiation of a thin-film Seemann-Bohlin focusing diffractometer.[3]

The technique of ion channeling and backscattering has been used to determine the lattice location of the implanted As ions as well as the orientation of the implanted region with respect to the unimplanted bulk material. The technique is well documented in the literature.[6] A 2-MeV He-ion beam is aligned with the atomic rows of the single crystal and the strong reduction of the backscattering He-ion yield for axial alignment is recorded. The dechanneling process is strongly sensitive to lattice disorder. The energy dependence as well as the angular dependence of the dechanneling yield will provide information on the defect structures present in the implanted region[7] and on the interface structure between implanted and unimplanted regions.[4] In order to get information on the interface region the angular yield curve is not only recorded for the implanted ions and host atoms in the implanted region but also for the host atoms in the region adjacent to the implanted layer. The energy windows used for these experiments are indicated for the spectra presented in Fig. 1.

Randomly aligned and $\langle 111\rangle$-aligned backscattering energy spectra have been measured as a function of the implanted As-ion concentration. Only one example of such spectra is presented in Fig. 1 for 15 at.% As. Helium ions backscattered from arsenic atoms are seen to be well separated in energy from those backscattered from vanadium atoms. Energy windows have been placed for the unimplanted bulk region (window No. 1), the implanted V region (No. 2), and the arsenic atoms (No. 3). The step in the random spectra in Fig. 1 determines the depth where the arsenic atoms are located (see depth scale). Further details of the $\langle 111\rangle$-aligned spectra will be discussed later.

Detailed angular scan measurements, recording the angular dependence of the normalized yields in windows No. 2 and No. 3, are shown in Fig. 2 for low arsenic concentrations. It is seen that for 0.5 at.% As [Fig. 2(a)], the minimum yield of the host, χ^h_{min}, is equal to the minimum yield of the arsenic atoms, χ^s_{min}. Thus the substitutional fraction F, defined by $F=(1-\chi^s_{\mathrm{min}})/(1-\chi^h_{\mathrm{min}})$, is equal to 1, i.e., all implanted arsenic atoms are on substitutional lattice sites. For 7.5 at.% As it can be seen [Fig.

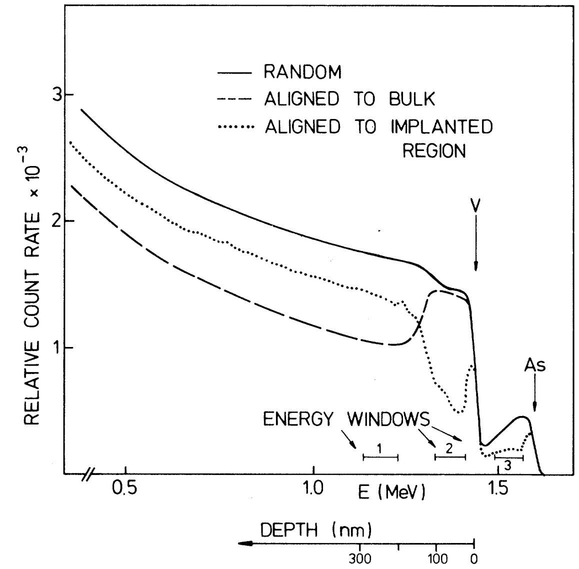

FIG. 1. Typical channeling and backscattering energy spectra for a high-dose (15 at.%) arsenic ion implantation in a vanadium single crystal. ⟨111⟩-aligned spectra are shown for axial alignment with the implanted region (dotted curve) and for axial alignment with the bulk (dashed curve).

2(b)] that the critical angle $\psi_{1/2}$ is narrower and $\chi^s_{\min}$ is larger than the corresponding values for the host crystal. A similar narrowing had been observed previously for Se ions implanted into vanadium.[8] Two models had been discussed in Ref. 8 for a possible explanation: (a) coherent precipitation of Se atoms, and (b) formation of a Se-vacancy defect complex.

For As concentration of 14 at.% and above, the minima of the angular yield profiles from energy windows No. 1 and No. 2 could no longer be found at the same tilt angle, ψ, but were displaced by a value $\Delta\alpha$. $\Delta\alpha$ changes with ϕ, the angle between the tilt plane and one of the three (110) planes present. The maximum value for $\Delta\alpha$ was found for $\phi = 90°$. For this case the tilt plane is perpendicular to a (110) plane, which will be called the slip plane. The maximum value of $\Delta\alpha$ will then be called the angle of rotation. A typical demonstration of these results is presented in Fig. 3. $\Delta\alpha$ has a maximum for $\phi = 90°$ [Fig. 3(a)] and disappears for $\phi = 10°$ [Fig. 3(b)].

The dependence of the angle of rotation on ϕ for two different crystals is shown in Fig. 4. It is clearly seen that the angle of rotation increases steeply with the concentration of implanted arsenic between 14 and 21.5 at.%. Experimentally it could be verified that the total implanted area with a diameter of 4 mm had been rotated with respect to the bulk.

A further increase of the As concentration leads to a polygonization of the implanted layer. Thin-film x-ray diffraction revealed that a polycrystalline layer had formed having bcc structure with a lattice parameter of $a = 0.3035$ nm (a of V is 0.3026 nm).

Figure 5 provides a simple illustration of the results presented in Figs. 3 and 4. When we vary

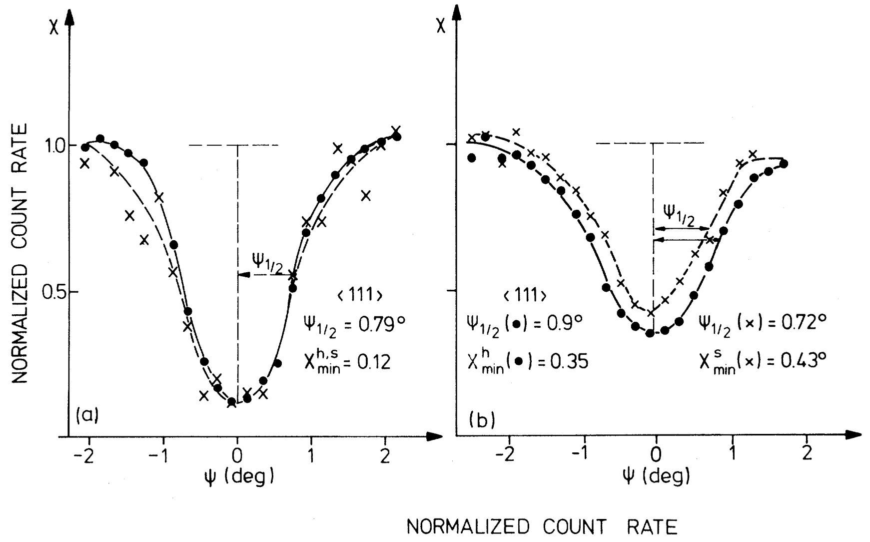

FIG. 2. Typical angular yield profiles through the ⟨111⟩-axial direction for the vanadium host lattice in the implanted region (circles) and for the implanted arsenic atoms (crosses). (a) 0.5 at.% As, (b) 7.5 at.% As. Incident beam: 2-MeV $^4\mathrm{He}^+$.

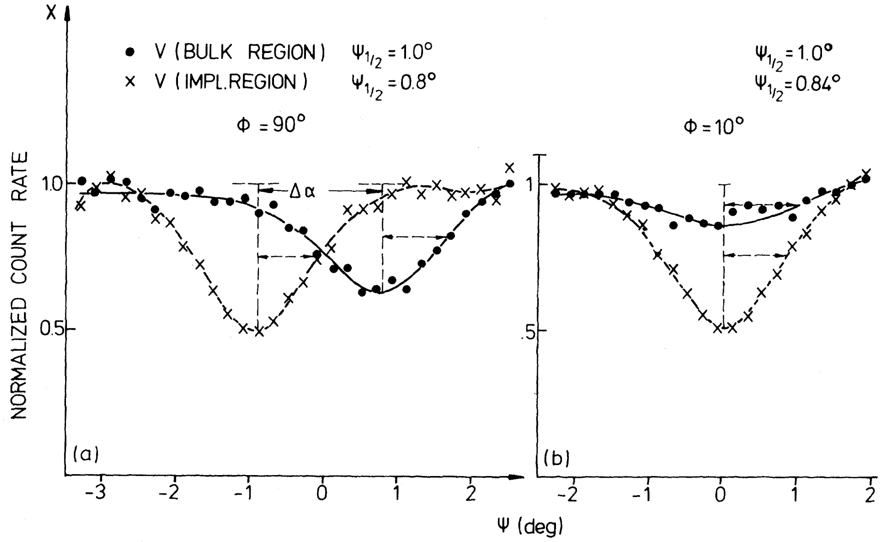

FIG. 3. Typical angular yield profiles through the ⟨111⟩-axial direction for the vanadium host lattice in the implanted region (crosses) and in the bulk region adjacent to the implanted region (circles). In (a) the tilt plane is perpendicular, in (b) 10° off the (110)-slip plane in the bulk.

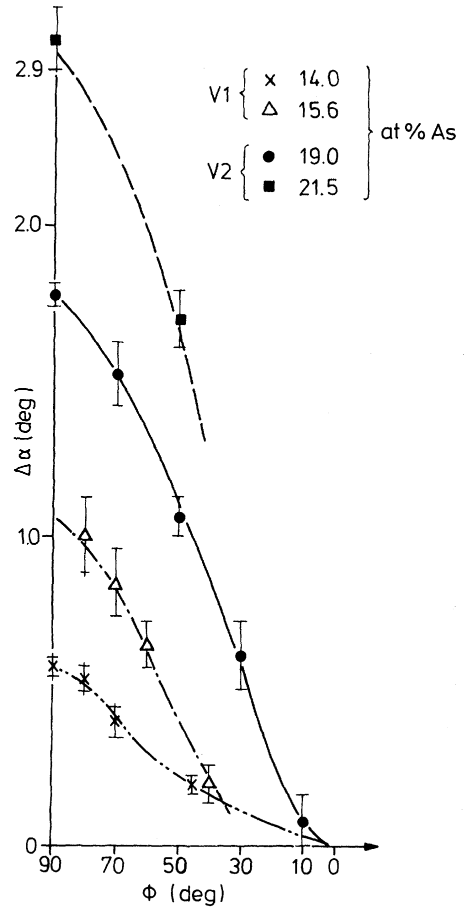

FIG. 4. Angular displacement of the minima, $\Delta\alpha$, vs ϕ, the angle between tilt plane and (110)-slip plane, with the As concentration as a parameter.

the tilt angle ψ in a plane at $\phi = 90°$, axial alignment is reached at $\psi = 0$ for the bulk region and at $\psi = -3°$ for the implanted region. If we choose a tilt plane at ϕ close to zero [in order to avoid channeling in the (110) plane at $\phi = 0°$] the minima in the angular scans are reached at $\psi = 0°$ for both the bulk and the implanted region. For this tilt geometry axial alignment and thus a low χ_{min} value is reached for the bulk whereas the rather high χ_{min} value in window 2 is due to some planar channeling in the implanted region.

Of course axial alignment with respect to the bulk as well as to the implanted region can easily be obtained. This is demonstrated in Fig. 1 showing typical ⟨111⟩-aligned backscattering spectra for axial alignment with the implanted layer (dotted line) and with the bulk (dashed line).

In order to explain the measured results we will follow similar arguments as already proposed in Ref. 4 for the case of thermally activated polygonization. Misfit strain fields are produced around the substitutional sites of the arsenic atoms and also between the implanted and the adjacent bulk region as a result of the different lattice parameter values. The tensile force component parallel to the surface normal may activate the slip systems which are known to be ⟨111⟩(100) and ⟨111⟩(211) for the bcc crystal structure [⟨111⟩ is the slip direction and (110) and (211) are the slip planes]. The implanted layer cannot slip freely as it is embedded in the single crystal. Thus the tensile force causes the slip direction to rotate towards the tensile axis which is the surface normal (see Fig. 5).

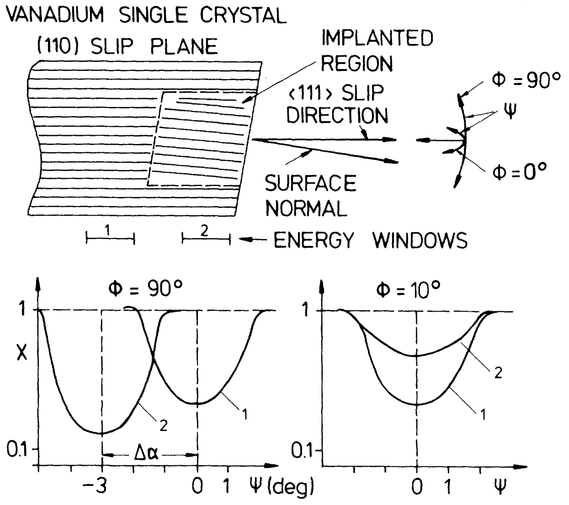

FIG. 5. Schematic drawing to illustrate the measured results. The tensile force component in the implanted region parallel to the surface normal *N* causes the slip direction to rotate towards *N*.

The results were reproduced for several V crystals with (111) surfaces and for one with a (110) surface. Whereas all (111)-surface crystals showed the rotation the (110)-surface crystal did not.

A further check is the following: If a slip mechanism is operative, then the Schmid factor[9] $\cos\lambda \cos\gamma$ should be largest for the activated (110) planes of the above-mentioned vanadium crystals with (111) surfaces. The angle λ between the slip direction and the surface normal is the same for each crystal with respect to three (110) planes and need not be considered. The angle γ between the surface normal and the normal of each of the three (110) planes should be smallest for the slip plane which is verified by the experiment. In one case a difference of 1°, causing about 20% difference in the resolved shear stress, was not recognized and in a second case a (211) plane was found to be the activated slip plane.

Under the assumption that the angle of rotation is proportional to the tensile force component, this force component seems to increase steeply with the As concentration (Fig. 3). The same result would be obtained on the assumption that the restraining force which hampers the motion of edge dislocations being the precondition for slip is lowered by the presence of As atoms. This would, however, be in contrast to the effect of solid solution hardening which is normally observed for alloys. Small atomic displacements ($\cong 0.015$ nm) of the foreign atoms from their lattice sites, probably due to coherent precipitation, may be a necessary precondition for the slip mechanism observed during the ion implantation process. This is supported by the Se-ion implantation experiment, where at 10 at.% Se the angle of rotation was found to be 0.6°. Increasing the Se concentration led to an amorphization of V.

In summary, a new implantation effect has been observed where the implanted region changes its crystal orientation with respect to the orientation of the bulk single crystal. The mechanism for this effect can be interpreted by the assumption that strain fields at the interface between implanted and unimplanted region and/or misfit strain fields around the As atoms activate the slip systems for the bcc structure. Only one slip system was found to be activated for each crystal, indicating that the process is still in stage I, where work hardening by intersecting slip planes does not yet occur. As the implanted region is embedded in the single crystal the slip direction will rotate towards the tensile force vector which is parallel to the surface normal. The effect has to be considered when the channeling technique is used for defect and lattice location analysis in high-dose-implanted structures.

---

[a] On leave from Nuclear Physics Department, Atomic Energy Establishment, Nuclear Research Center, Cairo, Egypt.

[1] J. M. Poate and A. G. Cullis, in *Treatise on Materials Science and Technology,* edited by H. Herman (Academic, New York, 1980), Vol. 18, p. 85.

[2] O. Meyer, in Ref. 1, p. 415.

[3] G. Linker, Nucl. Instrum. Methods **209**, 969 (1983).

[4] J. M. Lombaard, G. Linker, and O. Meyer, J. Less-Common Met. **96**, 191 (1984).

[5] M. Gettings, O. Meyer, and G. Linker, Radiat. Eff. **21**, 51 (1974).

[6] D. E. Gemmell, Rev. Mod. Phys. **46**, 129 (1974); W. K. Chu, J. W. Mayer, and M. A. Nicolet, *Backscattering Spectrometry* (Academic, New York, 1978), p. 127.

[7] Y. Quéré, Phys. Status Solidi **30**, 713 (1968), and Radiat. Eff. **28**, 253 (1976).

[8] H. W. Alberts, O. Meyer, and J. Geerk, Radiat. Eff. **69**, 61 (1983).

[9] See textbooks of physical metallurgy, e.g., J. D. Verhoeven, *Fundamentals on Physical Metallurgy* (Wiley, New York, 1975), p. 60.